Characterization of the nature of chemical species of heterogeneous Ziegler–Natta catalysts for the production of HDPE

Carlos R. Wolf [a], Maria Madalena de Camargo Forte [b], João Henrique Z. dos Santos [c],*

[a] Ipiranga Petroquímica, Departamento de Desenvolvimento de Produto, BR 386 Rod. Tabaí/Canoas, km 419, Triunfo 95853-000, Brazil
[b] UFRGS, Escola de Engenharia, Laboratório de Materiais Poliméricos, Rua Osvaldo Aranha 99, Porto Alegre 90035-190, Brazil
[c] UFRGS, Instituto de Química, Av. Bento Gonçalves 9500, Porto Alegre 91501-970, Brazil

Abstract

Highly active Ziegler–Natta (ZN) catalytic systems are used in slurry polymerization technology for high density polyethylene (HDPE) production. The nature of the active sites presented in the ZN catalyst influences the polyethylene properties. In this work, Ziegler–Natta heterogeneous supported catalysts were synthesized from $TiCl_4$ and magnesium ethylate with $MgCl_2$ in situ generation. It was observed that annealing time and temperature significantly influenced the catalytic activity. The non-annealed catalyst (ZNST) and the annealed catalyst (ZNT) presented the highest and the lowest catalyst activity, respectively. The ZNST and ZNT catalysts are amorphous solids and both have approximately the same surface area and particle size. By the catalyst chemical compositions, determined through different techniques, it was possible to conclude that thermal treatment (annealing) increases the Ti percentage and titanoxane sites in the catalyst. A structure was proposed for the titanoxane site different of that obtained in the $MgCl_2$ chloride addition using $TiCl_4$. ZNT catalyst with titanoxane active sites produces HDPE with high molecular weight while ZNST has different active sites, including titanates, and produces HDPE with low molecular weight.
© 2005 Elsevier B.V. All rights reserved.

Keywords: HDPE; Slurry; Ziegler–Natta catalyst; Ethylene polymerization; Titanium catalyst

1. Introduction

The Ziegler–Natta (ZN) catalyst has been used in the olefin polymerization since its discovery in 1950 [1–3]. Heterogeneous ZN catalysts are the main systems among polyolefin catalysts and they are responsible for the production over tens of million tonnes of polyethylene per year. The process type besides the control of the polymerization conditions allows products with special properties to be obtained, which has been motivating the continuous study of these catalysts until now [4–9]. The chemical composition of the ZN active sites influences the polymer properties and the characterization of active sites and the knowledge of their reactivity is very important in order to design new materials.

In the present work, heterogeneous ZN catalysts were synthesized based on the $MgCl_2$ in situ generation. The resulting catalysts were characterized and evaluated in bench polymerization reactor to produce high density polyethylene (HDPE) by means of the slurry process [10,11]. The chemical nature of these catalysts was correlated with the characteristics of HDPE obtained with certain active sites [12–16].

2. Experimental

2.1. Materials

All the reagents and catalysts were manipulated by the Schlenk Technique. Magnesium ethylate was purchased from Sivento; $TiCl_4$ and triethylaluminum (TEA) from Akzo Nobel; Exxsol D30 from Exxon Chemicals; hexane from

---

* Corresponding author. Fax: +55 51 3316 7304.
 E-mail address: jhzds@iq.ufrgs.br (J.H.Z. dos Santos).

Phillips; ethylene, hydrogen and nitrogen from Copesul and argon from White-Martins.

2.2. Catalyst preparation

The preparation of five heterogeneous Ziegler–Natta catalysts was based on the Hostalen Technology [10,11]. All catalysts were synthesized from the reaction between $TiCl_4$ and magnesium ethylate with $MgCl_2$ in situ generation. The Ti/Mg ratio was the same in all preparations. In the final step, one catalyst was not annealed (ZNST) and the four other catalysts were annealed at different annealing time and temperature.

2.3. Catalysts characterization

2.3.1. Elemental analysis

After sample digestion in H_2SO_4, Ti was oxidized with H_2O_2 and analyzed by visible spectrophotometry ($\lambda = 410$ nm) in a Lambda 2 spectrophotometer from Perkin-Elmer. The determination of the Ti^{3+} content was carried out using a solution of well-known concentration of Ce sulphate. The Cl amount was determined by the classic method of precipitation of AgCl with $AgNO_3$. Mg was determined by titrometry of the catalyst acid solution with EDTA.

2.3.2. Gas chromatography

The ethoxy groups ($-OCH_2CH_3$) of the catalysts were indirectly evaluated by ethanol released from the catalyst hydrolysis. The qualitative and quantitative analyses of ethanol and ethyl chloride was proceeded using a HP 6890 gas chromatographer equipped with a PMHS and a flame ionization detector (FID) and MSD5973N mass detector.

2.3.3. Rutherford backscattering spectrometry (RBS)

Metal loading in catalysts were determined by RBS using He^+ beams of 2.0 MeV incident on homogeneous pellets. During analysis the base pressure in the chamber was kept in the 10^{-7} mbar range using membrane (to prevent oil contamination of the sample) and turbodrag molecular pump. The method is based on the determination of the number and the energy of the detected particles, which are elastically scattered in the Coulombic field of the atomic nuclei in the target. For an introduction to the method and applications of this technique the reader is referred elsewhere [17,18].

2.3.4. X-ray photoelectron spectroscopy (XPS)

The X-ray photoelectron spectra (XPS) were obtained on a PHI 5600 Esca System (Φ Physical Eletronics), using monochromated Al Kα radiation (1486.6 eV). Spectra were taken at room temperature in low resolution (pass energy 235 eV) in the range of 1000–0 eV in the case of the survey spectrum and in high-resolution (pass energy 23.5 eV) modes for the Ti (2p) region.

The samples were mounted on an adhesive copper tape as thin films. Samples were prepared in a glove box, transferred under nitrogen atmosphere and then evacuated at 10^{-6} Torr by a turbomolecular pump in an introduction chamber for 90 min. During data collection, the ion pumped mass chamber was maintained at $5 < 10^{-9}$ Torr. Each sample was analyzed at a $75°$ angle relative to the electron detector. Normally 50 scans were signal averaged for selected binding energy windows and processed by the software supplied by the manufacturer. Neutralizer environment was 21.5 mA.

Binding energies were charge-referenced to the $MgCl_2$ Mg (2p). Three measurements per sample were made, and the reproducibility of the XPS analysis was confirmed. For each of the XPS spectra reported, an attempt has been made to deconvulate the experimental curve in a series of peaks that represent the contribution of the photoelectron emission from atoms in different chemical environments. These peaks are described as a mixture of Gaussian and Lorentzian contributions in order to take into account the effects of the instrumental error on the peak shape characteristic of the photoemission process. Estimation of surface atomic ratios was based on integrated areas and calculated atomic sensitivities factors, which were empirically derived from the electron energy analyzer supplied by Perkin-Elmer: O (1s), 5.148; Cl (2p), 5.161; Ti (2p) 12.741; Mg (2p) 0.809.

2.3.5. Diffuse reflectance infrared Fourier transform spectroscopy (DRIFTS)

The solid catalysts were analyzed as powder in a DRIFT accessory, equipped with sampling cup. The spectra were recorded at room temperature on a Bomem MB-102 Spectrometer, coadding 200 scan at resolution of 4 cm^{-1}. The spectra were collected as reflectance units and transformed to Kubelka–Munk (KM) units. All the measurements were performed at nitrogen atmosphere.

2.3.6. Physical properties of the catalysts

In order to get catalyst physical properties, the following analyses were carried out. Scanning electronic microscopy (SEM) analyses were performed using a DSM-940 Zeiss instrument operating at 5 kV. Samples were prepared by vaporization of carbon on the catalyst sample (20 μm thickness) by sputtering technique. Image magnifications varied from 200 to 500. The X-ray diffraction (XRD) analyses were performed in a Rigaku (DMAX 2200) difractometer equipped with a Cu tube and secondary monochromator, theta–theta Ultima goniometer and scintillation (NaI (Tl)) detector. Samples were prepared in glove box and pressed between mylar films. Particle size distribution analysis by laser light scattering (Malvern mastersizer microplus), and surface area by applying the Braunauer, Emmet and Teller (BET) method (Bell Belsorp 285A) (Bell). The size and the distribution of the microporos were calculated by Barret, Joyer and Halenda (BJH) method.

2.4. Bench polymerizations

Polymerization reactions in laboratory were made using a 1.5 L inox steel reactor. The reactor was fed with hexane, followed by TEA, the catalyst and H_2, according to required pressure. The polymerization was kept for 2 h starting from the stabilization of the temperature and control of the ethylene pressure. At the end, the reactor was discharged, and the powder polymer was filtered and dried.

2.5. Polymer characterization

Melting temperatures (T_m) were determined using a TA Instruments 2920 differential scanning calorimeter (DSC), according to ASTM D 3417/97 and ASTM D 3418/97. Two scans were performed, but only the results of the second scan are reported here. The heating rate was 10 °C/min in the temperature range from 30 to 200 °C, and the analysis was done under nitrogen atmosphere. MFR (melt flow rate) was obtained with a MP-E plastometer from Göttfert.

3. Results

3.1. Studying some parameters in catalyst synthesis

The addition rate of $TiCl_4$ to $Mg(OEt)_2$ was carefully established, since visually heterogeneous solids could be easily obtained. Once this parameter was controlled, the influence of annealing temperature and time on catalyst activity in ethylene polymerization was evaluated (Table 1).

According to Table 1, the highest activity was observed in the system, which was not annealed. All the catalysts, which had undergone a thermal treatment exhibited lower catalyst activity. Systems were shown to be dependent on annealing temperature and time: the higher the annealing temperature or time, the lower is the catalyst activity. Based on these results, it was decided to follow this work with the catalyst with very different activities, which could indicate differences in terms of chemical composition and HDPE properties. Therefore, catalyst prepared at conditions 1 (ZNT) and 5 (ZNST) were chosen.

Table 1
Catalyst activity as function of annealing during the catalyst synthesis

Experimental condition	Tempering temperature (°C)	Time (h)	Catalyst activity (g/mmol Ti h)
1	120	60	180
2	120	40	300
3	130	40	260
4	110	60	350
5	0	0	560

Polymerization at 85 °C (2 h), with TEA, Al/Ti ratio = 50, ethylene pressure = 6.2 bar and H_2 pressure = 1.26 bar.

Table 2
ZNST and ZNT chemical composition determined by wet methods and GC

Catalyst	Mg	Cl	Ti	–OCH_2CH_3
ZNST (not annealed catalyst)	1.0	2.3	0.3	0.5
ZNT (annealed catalyst)	1.0	3.4	1.3	≈0

3.2. Characterization of the catalyst sites

It is worth emphasizing that the catalysts were analyzed before the reduction with the cocatalyst. Table 2 presents elemental analysis in terms of Ti, Mg and Cl, determined by wet methods, and ethoxy amount, measured by GC, of ZNT and ZNST catalysts. In order to simplify the discussion, the chemical composition was expressed in the form of Mg:Ti:Cl ratio.

According to Table 2, catalyst annealing increases the relative amount of Ti and Cl amount in the catalyst by the reduction of ethoxy groups. Annealing process modifies the nature of the sites of the catalyst. Additional analysis of the chemical composition was proceeded by two direct techniques RBS and XPS. Fig. 1 shows a typical RBS spectrum of these catalysts. The plateaus corresponding to the elements constituents, O, Mg, Cl and Ti are well defined.

A representative survey spectrum of ZNT catalyst is presented in Fig. 2. All constituent atoms of the catalyst (Mg, Ti, Cl, O and C) were observed in the XPS sampling depth (approximately 3 nm).
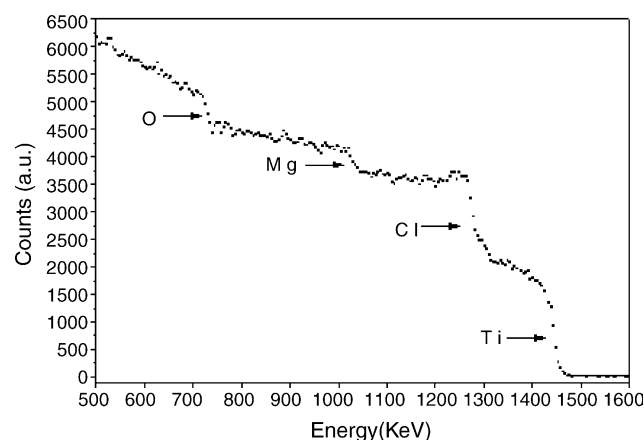

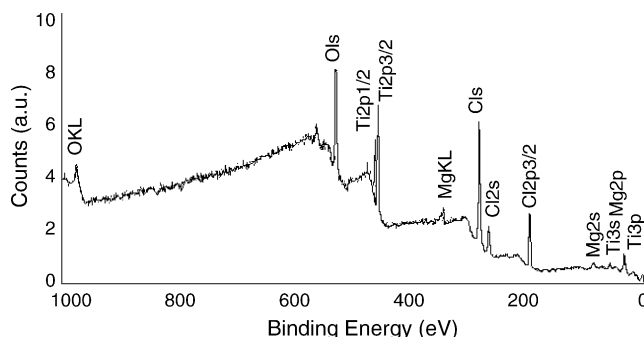Fig. 1. Typical RBS spectrum of ZNT.

Fig. 2. XPS survey spectrum of catalyst ZNT.

Table 3
ZNST and ZNT chemical composition determined by RBS and XPS

Catalyst	Technique	Mg	Cl	Ti	O
ZNST (not annealed)	RBS	1.0	1.5 ± 0.4	nd	0.3 ± 0.1
	XPS	1.0	1.5	0.1	1.0
ZNT (annealed)	RBS	1.0	1.6 ± 0.5	1.3 ± 0.6	3.2 ± 1.1
	XPS	1.0	1.7	1.7	4.8

nd, not determined.

Data from RBS and XPS were employed to obtain elemental analysis of these catalysts (Table 3).

According to Table 3, the results obtained by RBS and XPS show that ZNT catalyst has higher concentration of titanium and oxygen than ZNST, confirming the results obtained previously. No differences could be observed regarding the chlorine content. It is worth noting that comparing data from both techniques, values measured by RBS are systematically lower than those obtained by XPS.

In the case of RBS, the reach of 2.0 MeV He$^+$ ions in the support would be in the range of micrometers. On the other hand, the XPS measurable region is estimated roughly as 5 nm in depth. Therefore, XPS is more sensible to the uttermost surface composition, where the relative contribution of O and Ti atoms are much more important. In spite of the numeric differences between both techniques, grafted metal content showed the same trend among the different supported catalysts.

The Ti 2p XPS core-level of ZNST is shown in Fig. 3. Ti 2p core-level spectrum of the catalysts presents a doublet centered at 458.5 and 464.3 eV due to spin–orbit coupling of the 2p electrons of Ti and can be attributed to 2p$^{3/2}$ and 2p$^{1/2}$ photoelectrons, respectively.

Table 4 presents results of binding energy (BE) for Ti (2p$^{3/2}$) region and full width at half maximum intensity (FWHM) of ZNST and ZNT.

BE close to 458.0 eV indicates that the oxidation state of the Ti species is +4. This result is logical since the catalysts were not activated with cocatalyst. It is worth noting that ZNST presents a smaller BE than ZNT catalyst, which
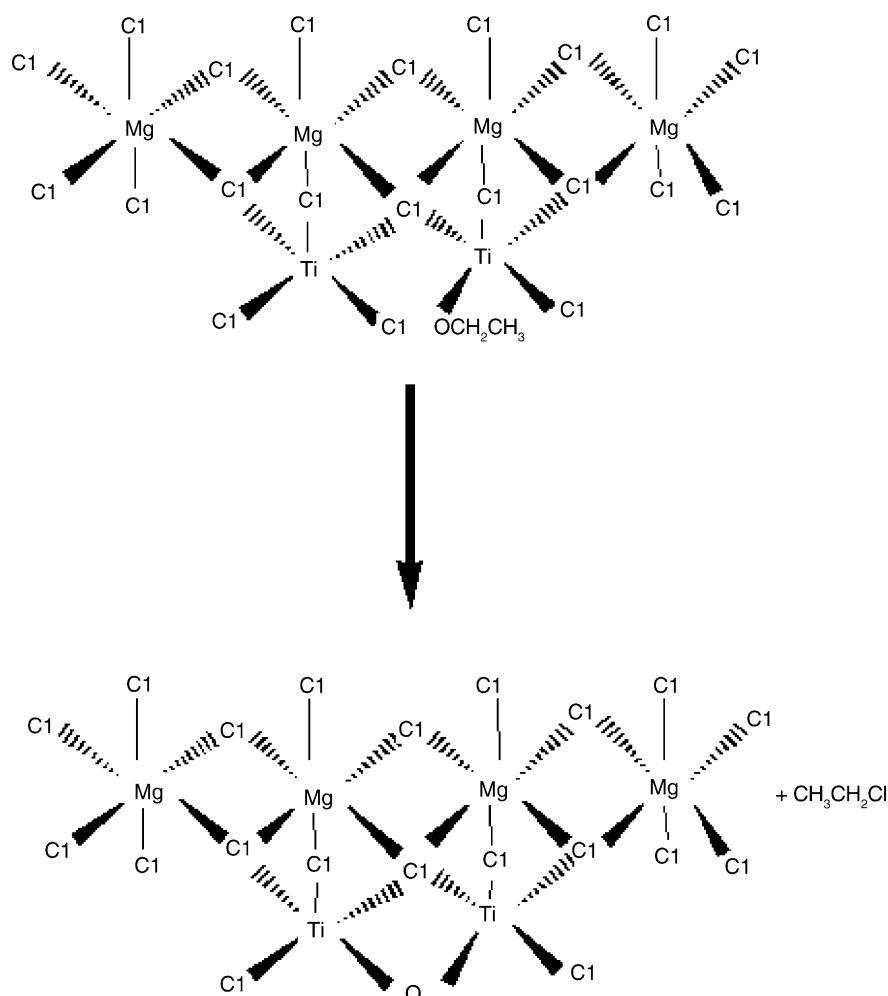
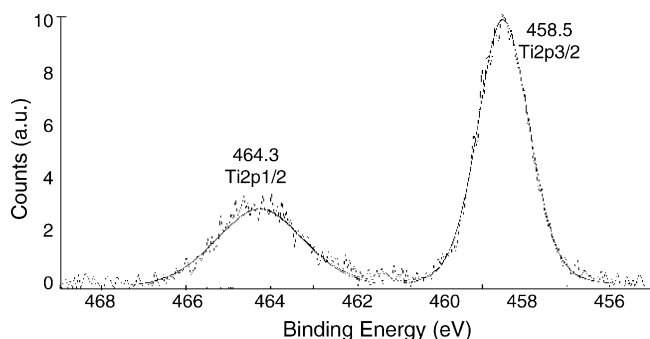Scheme 1. Proposed surface species before and after annealing.

Fig. 3. High-resolution XPS of Ti 2p region of ZNT. The small inserted peaks are the curve-fit components. The line with a visible noise component is the experimental raw data.

Table 4
Binding Energy (BE) of the Ti $2p_{3/2}$ peak of the catalyst determined by XPS

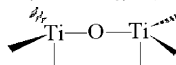| Catalyst	BE (eV)	FWHM
ZNT (annealed)	458.5	1.4
ZNST (not annealed)	458.3	2.3

FWHM, full-width at half maximum.

indicates that in ZNST catalyst, the Ti atoms lie in a more electron-rich environment after annealing.
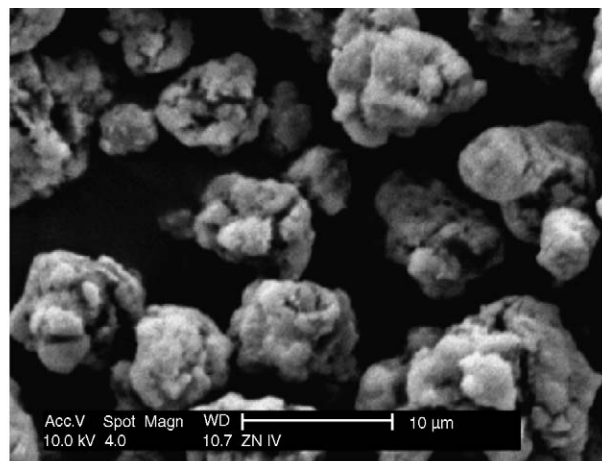
A correlation between catalyst activity and BE was already reported in the literature [19,20]. Catalyst with lower Zr BE in the case of supported catalyts presented higher catalyst activity [21]. In the present study, ZNST bears a lower Ti BE, which corroborates the results previously obtained in the polymerization evaluation (condition 5 versus condition 1 in Table 1). The active polymerization site is an ionic pair formed between a cationic metal center and the coordinated olefin. The acidity over the metal center might be tuned in order to be not too high and stabilize the interaction Ti^+-olefin, hindering the polymer chain propagation reaction, nor too low and therefore not engender the olefin coordination. It is worth noting that higher FWHM observed for ZNST suggest a more heterogeneous nature of Ti surface species.

Considering the results of chemical analysis, of ethoxy groups determination by GC, RBS and XPS results, it is possible to propose that there are oxygen sites on the surface of ZNT, which might not be present in ZNST. The latter might have sites with $-OCH_2CH_3$ groups in a significant concentration. These results took the proposition that non-annealed catalyst (ZNST) and annealed catalyst (ZNT) would have a considerable concentration of the sites represented in the Table 5.
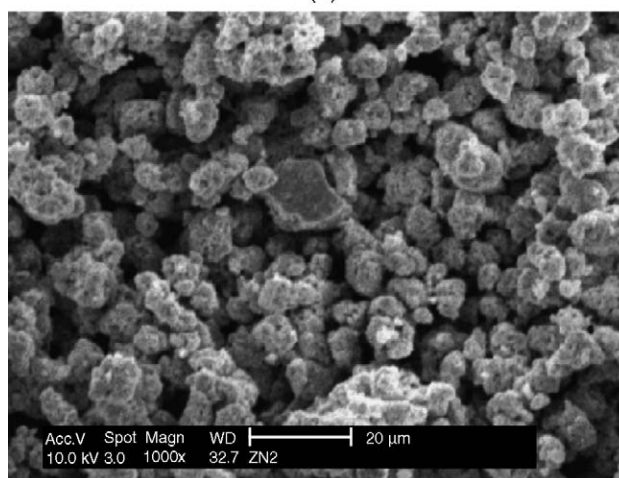

(A)

(B)

Fig. 4. Micrographies of ZNT (A) and ZNST (B) obtained by SEM.

For confirmation, additional analysis was proceeded by GC–MS. Exssol D 30 used in ZNT and ZNST preparation was analyzed and the results are also presented in Table 5. It was found that ethyl chloride in Exssol D-30 was only present during ZNT preparation, confirming the hypothesis.

In other words, annealing in the catalyst synthesis transforms sites of the type—$Ti(OCH_2CH_3)_nCl_{4-n}$, chlorotitanate where n varies from 1 to 3, into titanoxane (Ti–O–Ti), with ethyl chloride elimination (Scheme 1).

In order to obtain more evidences of the titanoxane formation in ZNT, samples of both catalysts ZNST and ZNT were analyzed by DRIFTS. Basically, two regions were integrated from the spectra: AP1 and AP2. The AP1 area was integrated from 2800 to 3000 cm^{-1} and contains informa-

Table 5
Chemical species of the catalyst sites

Catalyst	Main surface sites	Ethyl chloride in solvent preparation (ppm)
ZNST (not annealed)	$Ti(OCH_2CH_3)_{4-n}Cl_{n(n = 1, 2 \text{ or } 3)}$ and other sites	≈ 0
ZNT (annealed)	Ti—O—Ti and other sites	200 ± 100

Table 6
Temperature effect in AP2/AP1 ratio

Temperature (°C)	AP2/AP1	
	ZNT	ZNST
25	234 ± 29	85 ± 5
60	269 ± 3	316 ± 79
120	523 ± 25	1.358 ± 76

tion of the ν(C–H) stretching of the group chlorotitanate or titanate $[Ti(OCH_2CH_3)_{4-n}Cl_n]$, where n varies from 0 to 4. The AP2 area was integrated from 400 to 1000 cm^{-1} and it was related to titanoxane group absorption [22]. As it was not possible to get samples with the same thickness, the P2/P1 ratio was calculated. The evaluations were carried out in argon atmosphere with different temperatures, 25, 60 and

120 °C. in order to evaluate if AP2/AP1 ratio increases as function of temperature. Table 6 presents the results.

A tendency of decrease of AP1 and increase of AP2 was observed as a function of temperature increasing, much more pronounced in the case of ZNST catalyst. That is an evidence for the titanoxane formation (AP2) starting from titanate consumption (AP1) and ethyl chloride release. These results suggest that the titanoxane formation increases with the annealing temperature.

3.3. Morphology, texture and other catalyst physical properties

Fig. 4 presents the micrographies of ZNT and ZNST catalysts obtained by SEM. It shows that the catalysts do not have regular form.
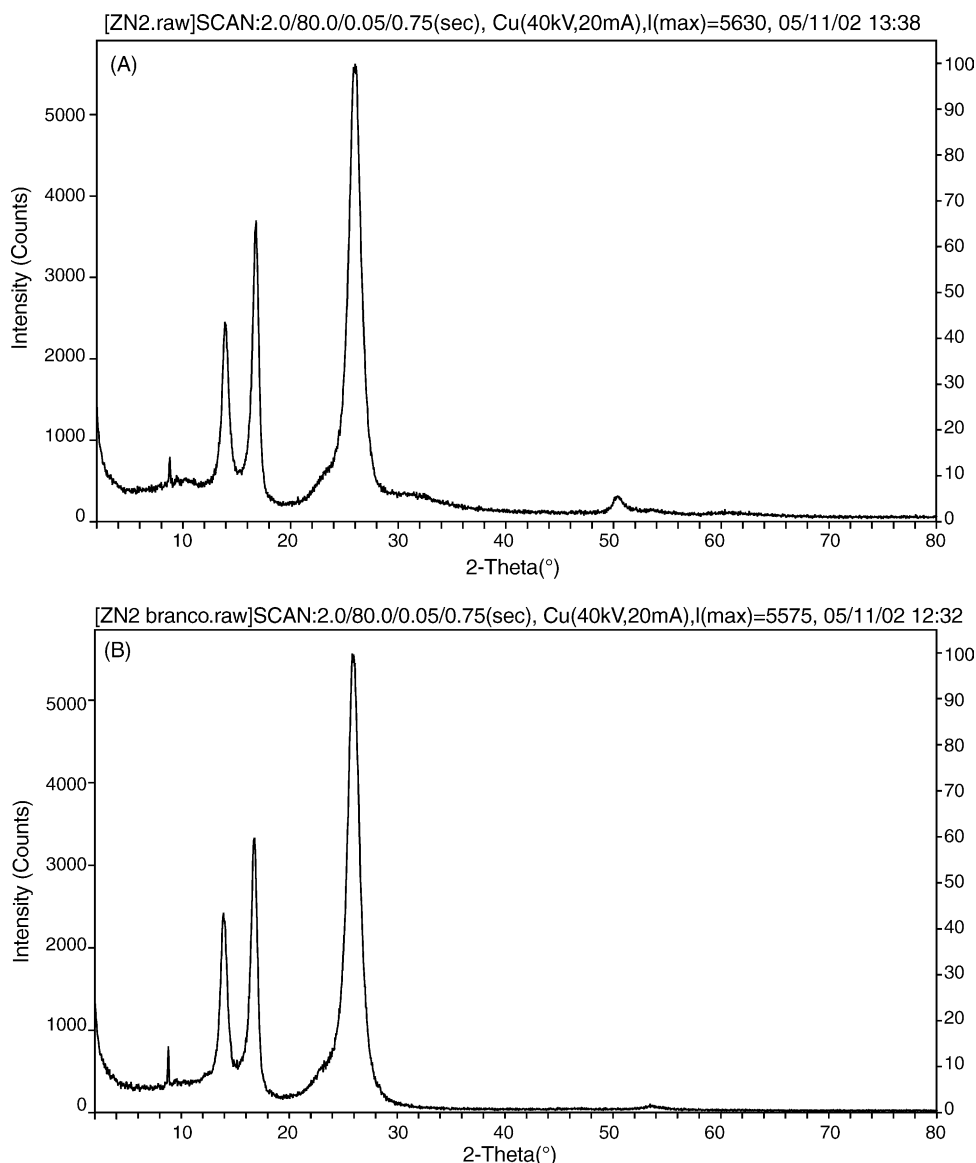

Fig. 5. DRX spectra of ZNST catalyst (A) and Mylar protective polyester film (B).
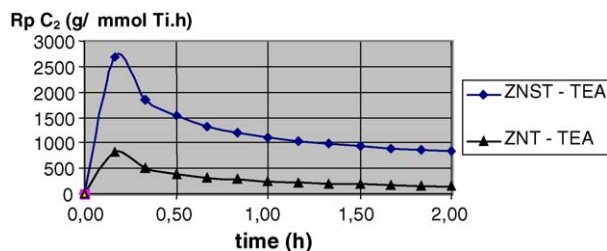
Fig. 6. Kinetics of ZNST and ZNT polymerizations.

The results from SEM and laser light scattering indicated that both catalysts is close to 10 µm. N_2 adsorption by the BET method showed that their surface area is about $125 \ m^2 \ g^{-1}$, the pore volume is approximately $0.4 \ cm^3 \ g^{-1}$ and the pore diameter about 11 nm. Crystalline peaks were not evidenced in the DRX analysis (Fig. 5). Only peaks relating to mylar could be observed, indicating that the catalysts are amorphous.

3.4. Catalyst evaluation

Fig. 6 shows the kinetic polymerization curves accomplished in a bench reactor for ZNST and ZNT catalysts. The reactions were accomplished at 85 °C, with TEA as cocatalyst and Al/Ti molar ratio of 50, employing ethylene and hydrogen pressures of 1.26 and 6.2 bar, respectively. For these reactions, it was considered the Ti^{3+} content determined by Ce sulphate method. Each polymerization was carried out for 2 h.

According to Fig. 6, both catalytic systems have maximum activity in the beginning of the polymerizations before the first 10 min and the same polymerization kinetic profile. Once again, ZNST has higher activity than ZNT.

The resulting polymers were characterized by the melting temperature (T_m) and melt flow rate (MFR) determination (Table 7).

From T_m results, it is possible to conclude the polymers obtained are HDPE. By MFR it is clear that the polymers have very different molecular weight. With ZNST is obtained a HDPE with low molecular weight while with ZNT the HDPE has high molecular weight. As the catalysts have differences between the active sites, related to the annealing process during catalyst preparation, it is possible to conclude that this modification allows obtaining different HDPE grades. It seems that the presence of Ti–O–Ti sites might generate more stable sites, which propagation rate is longer, allowing the polymer chain to grow further.

Table 7
Polymer analyses

Catalyst	T_m (°C)	MFR (190/5.0) g/10 min
ZNT	135	6
ZNST	134	44

4. Conclusions

In the present work heterogeneous, amorphous and mesoporous Ziegler–Natta catalysts were prepared with average particle size near to 10 µm and surface area of roughly $125 \ m^2 \ g^{-1}$. It was verified that annealing reaction during the preparation of these catalysts transforms some active sites of titanate or chlorotitanate type into titanoxane. The generation of such sites on the catalyst surface might be involved somehow both in the catalyst activity as in the polymer properties. This modification in the catalyst structure allows obtaining high density polyethylene with different molecular weight.

References

[1] L.L. Böhm, Chem. Ing. Tech. 56 (1984) 674.
[2] R. Franke, L.L. Böhm, W. Strobel, G. Thum, U. Wolfmeier, Transition, Proceedings of International Symposium on Transition Metals and Catalysis Polymerization, 2nd Meeting Date (1988), Publisher Cambridge University Press, Cambridge, 1986, pp. 428–437.
[3] L.L. Böhm, P. Goebel, P.R. Schöneborn, Die Angewandte Makromolekulare Chemie 174 (1990) 189.
[4] F. López-Linares, A.D. Barrios, H. Ortega, A. Karam, G. Agrifolio, E. González, J. Mol. Catal. A: Chem. 179 (2002) 87.
[5] H.S. Cho, Y.H. Choi, W.Y. Lee, Catal. Today 63 (2000) 523.
[6] H.-K. Luo, R.-G. Tang, H. Yang, Q.-F. Zhao, J.-Y. An, Appl. Catal. A: Gen. 203 (2000) 269.
[7] M. Alizadeh, N. Mostoufi, S. Pourmahdian, R. Sotudeh-Gharebagh, Chem. Eng. J. 9 (2004) 27.
[8] B. Liu, K. Fukuda, H. Nakatani, I. Nishiyama, M. Yamahiro, M. Terano, J. Mol. Catal. A: Chem. 219 (2004) 363.
[9] K. Fukuda, B. Liu, H. Nakatani, I. Nishiyama, M. Yamashiro, M. Terano, Catal. Commun. 4 (2003) 657.
[10] B. Diedrich, K.D. Keil, Hoechst AG, US Patent 3,644,318, 1972.
[11] J. Berthold, et al., Hoechst AG, US Patent 4,447,587, 1984.
[12] L.L. Böhm, et al., The microreactor as a model for the description of the ethylene polymerization with heterogeneous catalysts, in: Transition Metals and Organometallics as Catalysts for Olefin Polimerization, 1988, pp. 391–403.
[13] L.L. Böhm, J. Berthold, R. Franke, W. Strobel, U. Wolfmeier, Ziegler polymerization of ethylene: catalyst design and molecular mass distribution, in: T. Keii, K. Soga (Eds.), Studies in Surface Science and Catalysis, vol. 25, Catalytic Polymerization of Olefins, Elsevier, Amsterdam, 1986, pp. 29–42.
[14] L.L. Böhm, J. Appl. Polym. Sci. 29 (1984) 279.
[15] W.H. Ray, Ber. Bunsenges. Physik. Chem. 90 (1986) 947.
[16] L.L. Böhm, D. Bilda, W. Breuers, H.F. Enderle, R. Lecht, The microreactor model-guideline for PE-HD process and product development, Ziegler catalysts, in: Fink, Mülhaupt, Brintzinger (Eds.), Springer-Verlag, Berlin Heidelberg, 1995, pp. 387–400.
[17] F.C. Stedile, J.H.Z. Dos Santos, Nucl. Instrum. Meth. B 136–139 (1998) 1259.
[18] F.C. Stedile, J.H.Z. Dos Santos, Phys. Stat. Sol. 173 (1999) 123.
[19] F. Garbassi, L. Gila, A. Proto, J. Mol. Catal. A: Chem. 101 (1995) 199.
[20] P.G. Gassmann, M.R. Callstrom, J. Am. Chem. Soc. 109 (1987) 7875.
[21] M.C. Haag, C. Krug, J. Dupont, G.B. Galland, J.H.Z. dos Santos, T. Uozumi, T. Sano, K. Soga, J. Mol. Catal. A: Chem. 169 (2001) 275.
[22] C.M. Whang, S.S. Lim, Bull. Korean Chem. Soc. 21 (2000) 1181.